

Heat Transfer of a Liquid-Solid Contact in a Subcooled Pool Boiling System*

(Transition-Type Boiling Regime and Minute Bubble Emission Boiling Regime)

Shigeaki INADA**, Yoshiki MIYASAKA***
and Masakazu SAKUMOTO****

This report describes liquid-solid contact behavior in the subcooled pool transition-type boiling regime and the minute bubble emission boiling regime, detected by a void probe that uses a series-resonance circuit. This probe can approach the heated surface within two to three micrometers. The liquid-solid contact state discussed in this report means the nucleate boiling state caused by liquid invasion or Leidenfrost state caused by liquid rush onto the dry part on the heated surface. The dried area on the heated surface was estimated on the basis of the void signal, and the relation between the dried area on the heated surface and the measured heat flux was clarified by introducing a nucleate boiling model.

Key Words: Phase Change, Heat Transfer, Liquid-Solid Contact, Void Signal, Subcooled Pool Boiling, Transition-type Boiling, Minute Bubble Emission

1. Introduction

It is known that in the transition regime of saturated pool boiling, heat flux decreases with increase of wall temperature because a dry part appears and spreads on the heated surface with increase of wall temperature. However, even though wall temperature increases, the heat flux remains constant or even increases under certain circumstances in subcooled boiling⁽¹⁾ because the dry part of the heated surface is more readily furnished with liquid than in saturated boiling. The regime in which heat flux remains nearly constant against increases of wall superheat is termed transition-type boiling regime in this report, and the regime in which heat flux increases with increasing wall superheat beyond burnout heat flux is termed the

minute bubble emission boiling regime, in order to distinguish it from the ordinary transition regime in saturated pool boiling.

The liquid-solid contact state discussed in this report is the nucleate boiling state caused by liquid invasion or Leidenfrost state caused by liquid rush onto the dry part on the heated surface. In order to clarify the heat-transfer mechanism in saturated or subcooled transition boiling, it is important to evaluate correctly the spread area of the dry part on the heated surface.

Honda et al.⁽²⁾ evaluated the relation of forces acting on a coalescent vapor bubble on the heated surface in the transition regime of saturated boiling, and obtained the relationship equation from which the dried area was deduced as a time mean value. Further, they calculated the heat flux from the estimated relationship equation and compared these values with the measured heat flux.

Inada et al.⁽³⁾ evaluated the dried area on the heated surface in the transition-type boiling regime of subcooled pool boiling by a mathematical model based on the mass-transfer mechanism of evaporation and condensation through a coalescent vapor bubble. They

* Received 11th November, 1986. Paper No. 86-2016 B

** Department of Mechanical Engineering, Gunma University, 1-5-1 Tenjin-cho, Kiryu, 376, Japan

*** Okawarakakoki Co., 2-1-17 Tsukiji, Chuo-ku, Tokyo, 104, Japan

**** Ishikawajima Harima Heavy Industries Co., 3-1-15 Toyosu, Koto-ku, Tokyo, 135-91, Japan

1958

reported that the time-averaged heat flux calculated from the change with time of the dried area agreed well with the measured heat flux.

These reports mentioned above involve a few assumptions in the calculation of the dried area on the heated surface. Thus, it is desirable to have some direct techniques for measuring the dried area.

Iida et al.⁽⁴⁾ detected void signals in a saturated pool transition boiling regime by a void probe incorporating a series-resonance circuit over a wide range of probe heights, starting from 0.05 mm. They estimated the dried area on the heated surface by extrapolating a distribution of the void fraction down to the heated surface, and discussed the liquid-solid contact. However it is inaccurate to estimate the dried area on the basis of the void fractions in the range of heights above 0.05 mm by extrapolation, because the distribution of the void fraction is not always linear in heights below 0.05 mm.

Nishikawa et al.⁽⁵⁾ detected the liquid-solid contact state on the heated surface by means of thermocouples welded on the heated surface through the test boiling liquid, and Honda et al.⁽²⁾ measured the void fraction in saturated boiling by means of a void probe applying a D. C. voltage and an optical method. As the result, Nishikawa et al. and Honda et al. pointed out that the use of the void probe was not so desirable method in detection of the liquid-solid contact state on the heated surface because the void fraction near the heated surface was sensitive to small changes in the height of the probe.

In an earlier report⁽⁶⁾, the state of vapor bubble generation in the same boiling regime as in this report was studied using the same void probe as that used by Iida et al.⁽⁴⁾, keeping a constant distance between the probe height and the heated surface. However, an estimation of the dried area on the heated surface based on the void signal has yet to be given, and the liquid-solid contact state and its heat-transfer mechanism in the minute bubble emission regime have yet to be fully clarified.

As a result of the above, in this report, using the same void probe method as that used by Iida et al., but with equipment to enable the probe to approach accurately the heated surface within two to three micrometers, the void fraction in a vertical direction to the heated surface was obtained, and the ratio of the dried area to the liquid-solid contact area on the heated surface was measured. The relation between the dried area and the measured heat flux on a locality of the heated surface was clarified by introducing a nucleate boiling model.

Furthermore, in the minute bubble emission boiling regime, the authors caught the void signals which

correspond to the period of the liquid-solid contact on the heated surface.

2. Experimental Apparatus and Procedure

The subcooled pool boiling apparatus and the structure of the probe used in this experiment are similar to those in the earlier report⁽⁶⁾, so explanations are omitted here.

The void signal detection circuit from the series-resonance circuit is shown in Fig. 1. The circuit consists of an oscillator, a coil having a self-inductance L , and a condenser composed of two conductors, one being a double probe and the other the heated surface. The resonance frequency and the self-inductance of the coil are in the range of 3 000 to 5 000 Hz and about five Henry, respectively. If there is a vapor bubble between the probe and the heated surface, the output voltage of the condenser fluctuates widely because of the large difference between vapor and liquid permittivities. The fluctuation of the output is amplified further and indicated on an oscillograph through the D. C. restoration and clipper circuits. The frequency response of the amplifier is flat from 0 to 5 kHz.

A double probe was used to determine the differences in the void signals with regard to location. One probe was set on the vertical line A above the central part of the heated surface, and the other on line B above the peripheral part 3 mm away from the center of the heated surface.

The double probe can be brought to within 0.002–0.003 mm of the heated surface by a magnifying device that uses a bimetal-type cantilever. The dis-

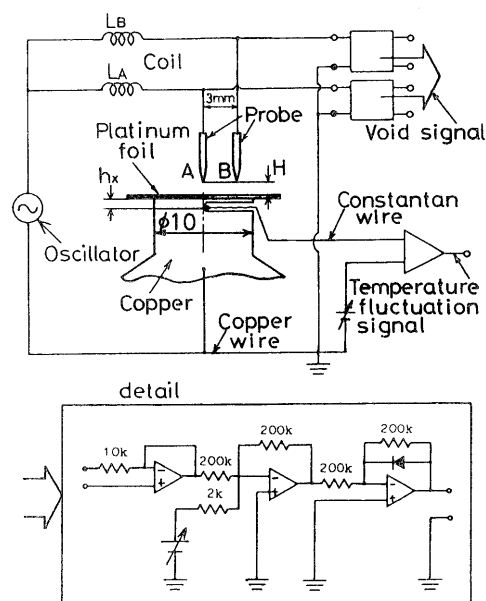


Fig. 1 Circuits for detecting void signal and temperature variation of the heated surface

placement of the micrometer required move the probe by 0.001 mm is 0.11 mm, and its minimum displacement is 0.01 mm.

The probe is made of a platinum wire 0.05 mm in diameter which is molded in a pyrex glass tube. The tip of the probe is about 0.1 mm diameter and is formed into a needlelike shape. It is not likely that the boiling heat transfer would be influenced by the disturbance which is caused by thrusting the probe into the coalescent vapor bubble, because heat transfer in the coalescent vapor bubble regime is mainly dominated by the autonomous behavior of the vapor bubbles, which are generated continuously at the root of the coalescent vapor bubble.

A thermocouple installed close to the uppermost surface of the copper cylindrical tip was used to detect the temperature variation of the heated surface. In order to minimize the distance from the very tip to the thermocouple, a hole of 0.5 mm diameter was drilled for mounting a thermocouple, and then the upper surface of the tip was shaved by a lathe. The distance from the top to the thermocouple was $h_x = 0.25$ mm. In addition, a platinum foil of 0.05 mm thickness was diffusion-bonded to this upper surface of the tip. The direct-current component of the temperature signal picked up by the thermocouple was suppressed by a standard voltage generator, and only the fluctuation component was amplified and recorded on an oscillograph. The temperature signal at the central part A of the heated surface was amplified so that the ratio was 3.8 K/cm.

3. Boiling Curve and Measured Regime

Figure 2 shows the boiling curve, that is, mea-

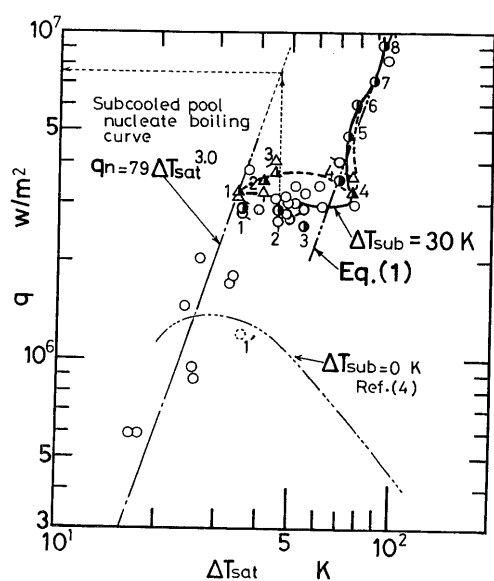


Fig. 2 Boiling curve and the measured boiling regime

sured heat flux q vs wall superheat ΔT_{sat} for subcooling ΔT_{sub} of 30 K. Data obtained at the central part of the heated surface are marked by the symbol \circ and connected by a solid line. Data at the peripheral part of the heated surface are marked by the symbol \triangle and connected by a broken line. The boiling regions numbered and marked by the symbol \bullet or \blacktriangle indicate where void signals were detected by a double probe. This boiling curve was obtained for a contaminated surface with scale-deposit after the first run, which required eight hours of boiling.

In the boiling region from 1 to 4, the heat flux remains nearly constant, even if the wall temperature rises, so this region was called the transition-type boiling regime in this report.

In region 4, a very thin vapor film appears on the entire heated surface and the state gradually proceeds to stable film boiling; however, if the heated surface contamination proceeds from the state of region 4, the heat flux increases abruptly and the state gradually enters region 5, where a number of minute vapor bubbles are rapidly emitted from the heated surface. Thus, the boiling region above region 4 is called the minute bubble emission regime.

The measured heat flux in this regime is proportional to the cube of the wall superheat. The relation is given by Eq. (1) and is shown by a two-dotted line in Fig. 2;

$$q = 11.1 \Delta T_{sat}^{3.0} \quad (1)$$

where q is in the unit of W/m^2 and ΔT_{sat} in K.

The chain line in Fig. 2 indicates the nucleate boiling curve which was obtained by summing up the data on subcooled pool nucleate boiling. The three-dotted line, which is the saturated boiling curve obtained by Iida et al.⁽⁴⁾, represents the conventional transition boiling curve.

4. Distinction of Liquid and Vapor Phases based on Void Signals and Definition of Void Fraction

Figure 3 shows an example of a void signal

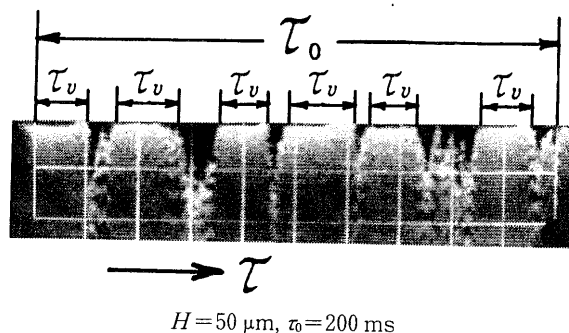


Fig. 3 Distinction of liquid and vapor phases based on void signals

1960

detected at a height of 0.05 mm from the heated surface for the region 1 of Fig. 2. Several wide-band signals indicate the vapor phase, implying that coalescent vapor bubbles form successively on the heated surface. Two to three signals standing up sharply with a short period indicate generation of nucleate boiling bubbles. This means that active nucleate boiling occurs in the superheated liquid film between coalescent bubbles and the heated surface. The dips of the void signal show the presence of the liquid phase.

In a pool boiling system, the void fraction f_v at an arbitrary height is defined as the ratio of the summation of all the τ_v contained in that sampling time to the sampling time $\tau_o^{(4)}$.

$$f_v = \frac{\sum \tau_v}{\tau_o} \quad (2)$$

In this study, only the wide-band signals of τ_v shown in Fig. 3 are considered to be signals indicating the presence of the vapor phase, since the active nucleate boiling signals can be assumed to be liquid-contact signals. In the limit when the probe approaches the heated surface, if the vapor phase signals are detected, this means that the heated surface is dry and if the nucleate boiling signals are detected, this means that the heated surface is wet. In the end, it is necessary to distinguish clearly vapor phase signal and nucleate boiling signal in order to estimate the ratio of the dried area to the heated surface area from the information based on the void signal (see Chapter 6). The sampling time is about 200 ms and the void fraction is obtained from the averaged value of several measurements under the same condition.

5. Void Signals and Void Fractions nearby Heated Surface

Figure 4 shows the void signals detected by chang-

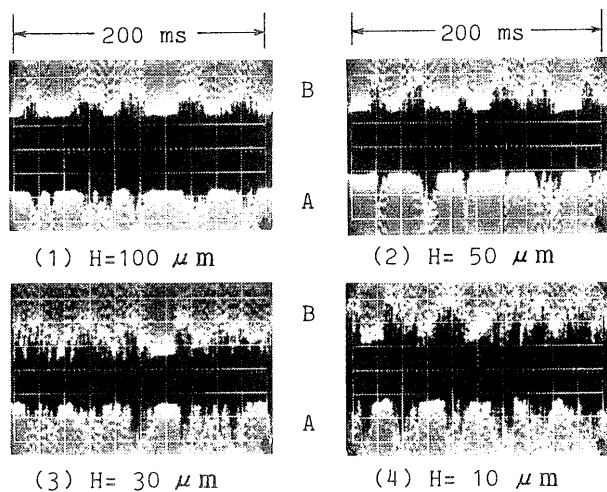


Fig. 4 An example of void signals measured for region 1 in Fig. 2

ing the position of the double probe in a vertical direction and keeping the electric input to the heated surface constant for region 1 in Fig. 2. Two signals on the vertical lines A and B in Fig. 1 are respectively recorded upwards from the bottom and downwards from the top on the oscillograph so that they are facing each other. At heights of the probe H exceeding 0.05 mm, the wide-band signals appear clearly and their durations are longer than the active nucleate boiling signals. On the other hand, at heights less than 0.05 mm, the active nucleate boiling signals occur nearly exclusively at location B. Therefore, it is clear that the probe must be set at heights less than 0.05 mm in order to detect liquid-solid contact on the heated

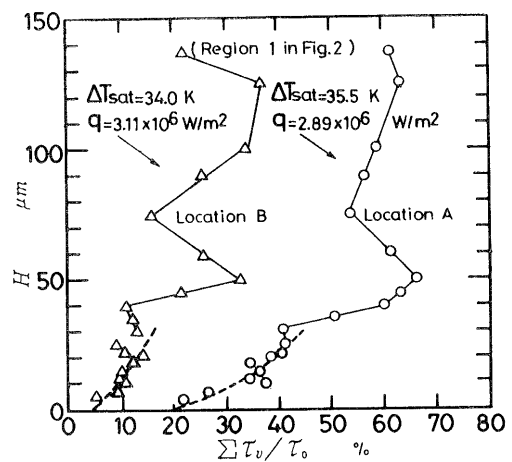


Fig. 5 Correlation between the height H and the void fraction measured for region 1 in Fig. 2

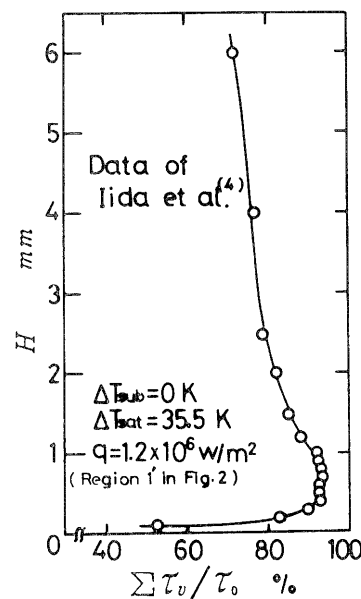


Fig. 6 Correlation between the height H and the void fraction obtained by Iida et al. for region 1' in Fig. 2

surface. Judging from the void signals at $H=0.01$ mm, it was found that the dry part appears mainly on the central part and the active nucleate boiling always occurs on the peripheral part of the heated surface.

Figure 5 shows the correlation between the height H and the void fraction for the region 1 of Fig. 2, which belongs to the burnout region. The void fractions are considered to be roughly 60 percent on A and 30 percent on B at heights exceeding 0.05 mm, though the data are very scattered. However, in the range of heights below 0.05 mm on both A and B, the void fraction decreases with decreasing H and reaches a value of about 20 percent and 5 percent, respectively, on the heated surface.

Figure 6 shows the void fractions obtained by Iida et al. for the region 1' of Fig. 2 over a wide range of heights from 0.05 mm. The same void fractions as ours are obtained at a height close to 0.05 mm.

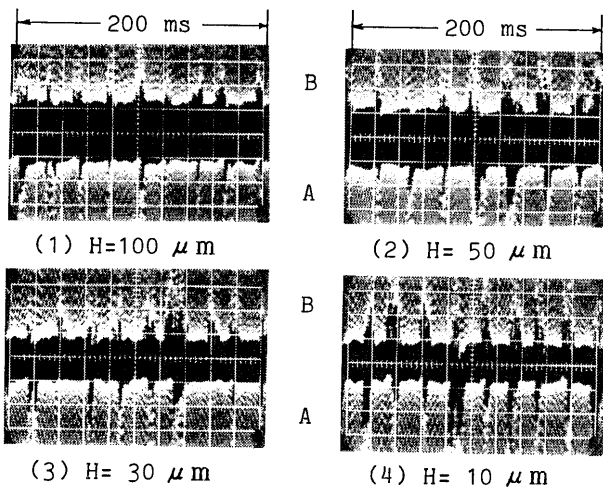


Fig. 7 An example of void signals measured for region 2 in Fig. 2

Though accurate predictions cannot be made in the height range below 0.05 mm from their results, both Figs. 5 and 6 show that the void fractions decrease with a decrease in H .

Figures 7 and 8 respectively show the void signals and the void fractions for the region 2 of Fig. 2. The wide-band signals appear clearly at a constant period, but the active nucleate boiling signals do not appear appreciably, even when the probe closely approaches the heated surface. The void fractions on both A and B increase rapidly and are distributed from 60 to 85 percent in the range of heights above 0.03 mm. However, in heights below 0.03 mm, the void fraction on B decreases with decrease in H , and reaches a value of about 42 percent on the heated surface.

Figures 9 and 10 respectively show the void signals and the void fractions for the region 3 of Fig. 2. In this boiling region, the coalescent vapor bubbles for-

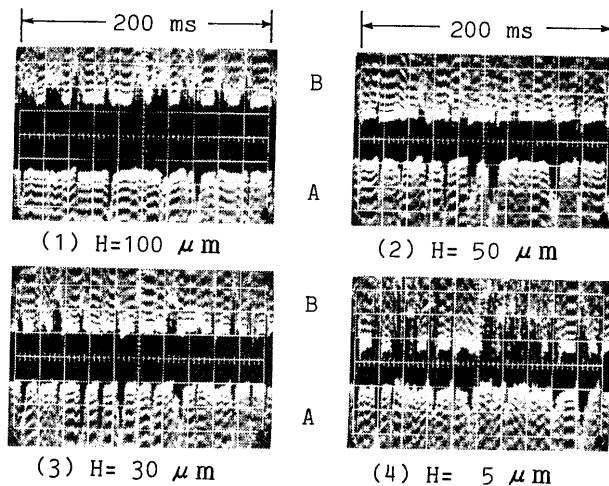


Fig. 9 An example of void signals measured for region 3 in Fig. 2

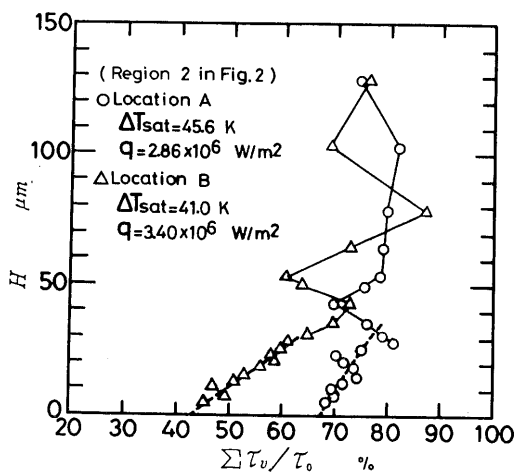


Fig. 8 Correlation between the height H and the void fraction measured for region 2 in Fig. 2

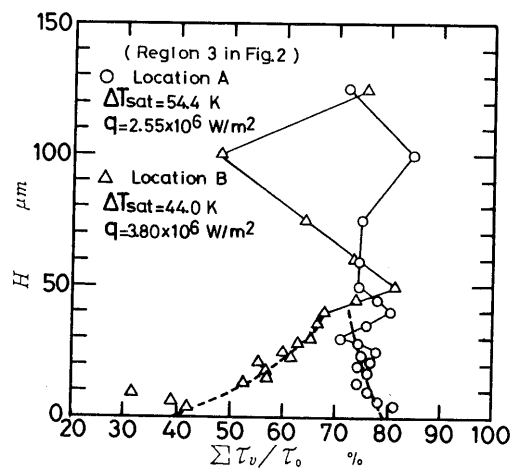


Fig. 10 Correlation between the height H and the void fraction measured for region 3 in Fig. 2

med on the heated surface are of such indeterminate shape that irregular-shaped wide-band signals appear at both A and B. No liquid-solid contact signals are recognized at A, but the duration of liquid-solid contact at B increases rapidly with decrease in H . Comparing the magnitude of the void fraction for region 2 with region 3, the void fraction for region 3 is higher at A and is lower at B than that for region 2, that is, the difference of void fractions on a locality of the heated surface is remarkable for region 3.

Figures 11 and 12 show void signals and the void fractions measured for the region 4 of Fig. 2. In this region, many irregularly-shaped, divided bubbles developed to cover the peripheral part of the surface⁽⁷⁾. As is evident at B in Fig. 11, the presence of the liquid phase becomes indistinct and the vapor phase always emerges. On the contrary, liquid-solid contact signals and wide-band signals appear at A intermittently,

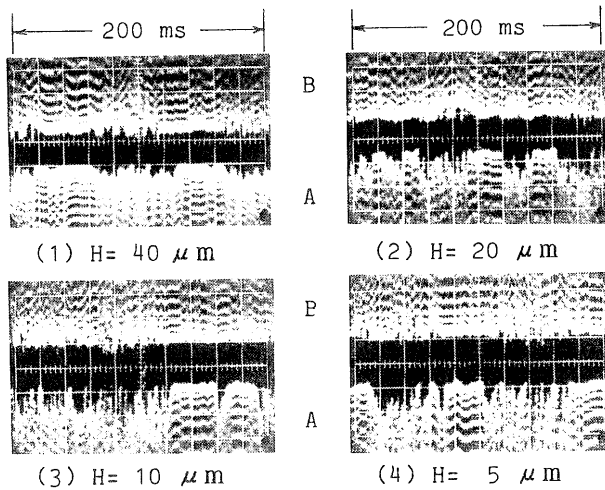


Fig. 11 An example of void signals measured for region 4 in Fig. 2

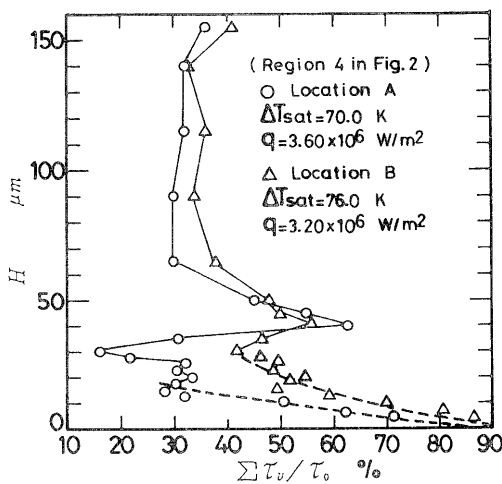


Fig. 12 Correlation between the height H and the void fraction measured for region 4 in Fig. 2

corresponding to the moment a number of minute bubbles are rapidly emitted from the heated surface.

According to Fig. 12, the void fraction at A is low in value, rather than that at B. When the wall superheat was increased by a few degrees above region 4, a number of minute bubbles were continuously emitted from the entire heated surface and only liquid-solid contact signals were detected.

Figure 13 shows the void signals detected by changing the position of the double probe in a vertical direction and keeping the electric input to the heated surface constant for the region 5 of Fig. 2. No difference in the void signals is recognized, even if the position of the probe is changed in a vertical direction. This means that the vapor bubble which is urged to detach from the heated surface passes forcibly through the subcooled liquid as is.

Figure 14 shows the void signals detected for the

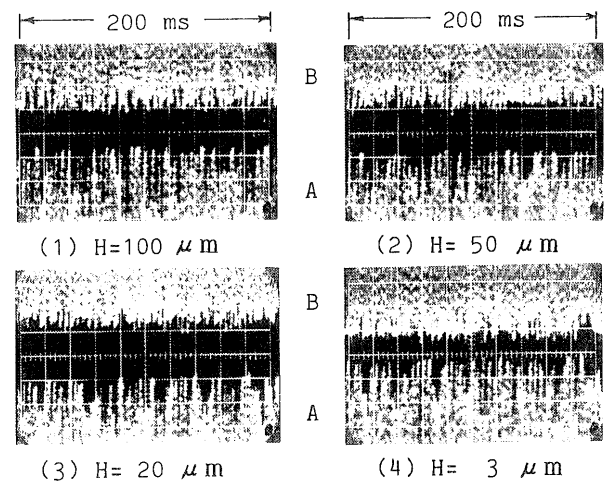


Fig. 13 An example of void signals measured for region 5 in Fig. 2

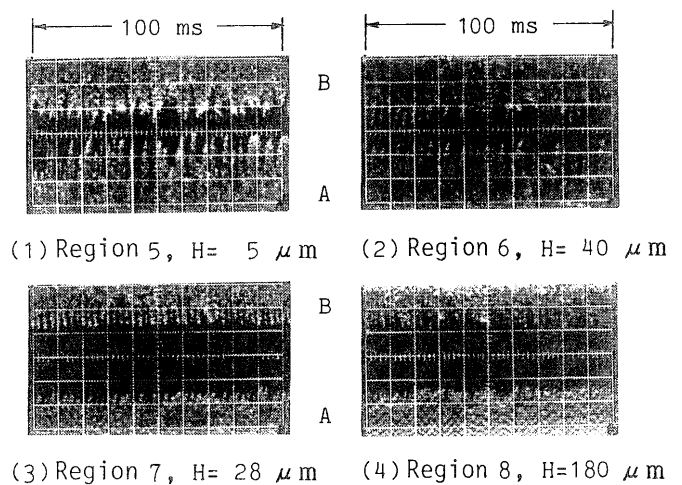


Fig. 14 An example of void signals measured for regions 5, 6, 7 and 8 in Fig. 2

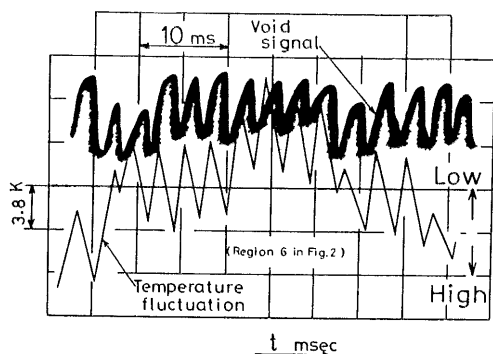


Fig. 15 An example of void signal and temperature variation measured at the same time for region 6 in Fig. 2

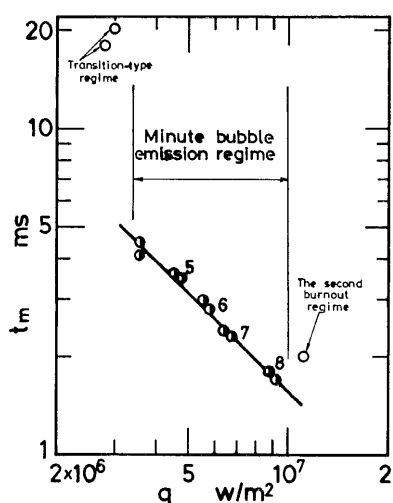


Fig. 16 Relationship between the liquid-solid contact period and the measured heat flux

regions 5, 6, 7 and 8 of Fig. 2. For regions 5 and 6, the period of the liquid-solid contact on B is a little shorter than that of A, but for regions 7 and 8, both the period and the phase of the void signals agree precisely, regardless of the locations A and B. The period of the liquid-solid contact becomes noticeably shorter with increase of heat flux.

Figure 15 shows an example of void signals and temperature variations measured at the same time for measured region 6 of Fig. 2. The variation period of void signal agrees with that of temperature. Judging from the results in Figs. 13-15, it can be considered that the period of the void signal detected corresponds to the period of the liquid-solid contact on the heated surface.

The periods t_m of the liquid-solid contact measured from the void signals are shown by symbol ● in Fig. 16 against the measured heat flux q . The period of the liquid-solid contact becomes short with increase

of the heat flux, and they have an inversely proportional relationship.

6. The Relation between the Void Fraction on the Heated Surface and the Time Mean Value of the Local Heat Flux

The broken lines shown in Figs. 5, 8, 10 and 12 show the distribution of the void fraction in the neighborhood of the heated surface. The void fraction on the heated surface was obtained by extrapolating the broken line down to the heated surface.

Denoting the void fraction on the heated surface by f_{gw} , the ratio of the time mean value of the dried area S_d to the area of the heated surface S_w can be roughly assumed by,

$$f_{gw} = \bar{S}_d / S_w \tag{3}$$

If it is assumed that the heat flux accompanied with the generation of vapor bubbles caused by liquid-solid contact maintains value q_n of a monotonous extension of the nucleate boiling curve shown in Fig. 2, the substantial heat flux \bar{q}_{th} in the transition-type boiling regime is expressed as

$$\bar{q}_{th} = (1 - f_{gw}) q_n = 79(1 - f_{gw}) \Delta T_{sat}^{3.0} \tag{4}$$

The substantial heat flux \bar{q}_{th} evaluated from Eq. (4) at measured regions 1, 2, 3 and 4 are plotted in Fig. 2 by symbols Q, ○, ◐ and ◑ for location A and △, ◒, ◓ and ◔ for location B, respectively. The value of \bar{q}_{th} agrees with the measured heat flux q within a ±15% error.

Equating two expressions, Eqs. (1) and (4), gives

$$\bar{S}_d / S_w = 0.86 \tag{5}$$

Therefore, in the minute bubble emission regime, it can be considered that 86 percent of the heated surface area is always drying; in other words, the void fraction f_g equals 0.86 regardless of the height of the probe.

7. Conclusions

The liquid-solid contact states in the transition-type boiling regime and in the minute bubble emission boiling regime for pool boiling at subcooling of 30 K are examined in detail by a direct technique using a void probe and by measurement of the temperature fluctuation in the heated surface. The conclusions from the experiment described above may be summarized as follows.

In the transition-type boiling regime, (1) the void probe must be set at a height below 0.05 mm in order to detect the liquid-solid contact state on the heated surface; and (2) the dried area on the heated surface was estimated on the basis of the void signal, and the relation between the dried area on the heated surface and the measured heat flux was clarified by

1964

introducing a nucleate boiling model.

In the minute bubble emission boiling regime,

(1) no difference in the liquid-solid contact signals was recognized, even when the height of the probe changed; (2) the void signals which corresponded to the period of the liquid-solid contact on the heated surface were detected; and (3) the measured heat flux was far beyond the burnout heat flux and was proportional to the cube of the wall superheat, but the boiling curve moves to a higher magnitude of wall superheat than that obtained in the conventional nucleate boiling.

A part of this investigation was supported by a grant from the Scientific Research Fund as appropriated by the Japanese Ministry of Education (Research grant No. 60550144).

References

- (1) Miyasaka, Y., Inada, S. and Izumi, R., *Int. Chem. Eng.*, Vol. 23, No. 1 (1983), p. 48.
- (2) Honda, H. and Nishikawa, K., *Trans. Jpn. Soc. Mech. Eng.*, Vol. 38, No. 305 (1972), p. 177.
- (3) Inada, S., Miyasaka, Y., Izumi, R. and Kobayashi, M., *Bull. JSME*, Vol. 25, No. 205 (1982), p. 1085.
- (4) Iida, Y. and Kobayashi, K., *Trans. Jpn. Soc. Mech. Eng.*, Vol. 36, No. 283 (1970), p. 446.
- (5) Nishikawa, K., Fujii, T. and Honda, H., *Trans. Jpn. Soc. Mech. Eng.*, Vol. 37, No. 297 (1971), p. 1018.
- (6) Inada, S., Miyasaka, Y., Sakumoto, S. and Chandratilleke, G. R., *Trans. ASME, Ser. C*, Vol. 108, No. 1 (1986), p. 219.
- (7) Inada, S., Miyasaka, Y. and Izumi, R., *Heat Transfer Japanese Research*, Vol. 11, No. 2 (1982), p. 42.